PCCP

Check for updates

Ordered assembly of non-planar vanadyl-tetraphenylporphyrins on ultra-thin iron oxide

Guglielmo Albani,[a] Luca Schio, [b] Francesco Goto,[a] Alberto Calloni, [*a] Alessio Orbelli Biroli, [c] Alberto Bossi,[d] Francesco Melone,[e] Simona Achilli, [e] Guido Fratesi, [e] Carlo Zucchetti,[a] Luca Floreano [b] and Gianlorenzo Bussetti [a]

Stabilizing ordered assemblies of molecules represents the first step towards the construction of molecular devices featuring hybrid (organic–inorganic) interfaces where molecules can be easily functionalized in view of specific applications. Molecular layers of planar metal-tetraphenylporphyrins (MTPP) grown on an ultrathin iron oxide [namely Fe(001)–$p(1 \times 1)$O] show indeed a high degree of structural order. The generality of such a picture is tested by exploiting non-planar porphyrins, such as vanadyl-TPP (VOTPP). These molecules feature a VO^{2+} ion in their center, with the O atom protruding out of the plane of the porphyrin ring. In this work, by employing diffraction, photoemission and X-ray absorption, we prove that non-planar VOTPP can nevertheless form a square and ordered superstructure, where porphyrin molecules lie flat with respect to the underlying substrate. *Ab initio* density functional theory simulations are used to elucidate the V=O bond orientation with respect to the iron substrate.

Introduction

Organic–inorganic interfaces are becoming nowadays more and more important in hybrid organic electronics[1,2] and spintronics[3,4] due to the possibilities offered by these molecules in terms of synthesis, functionalization, tunability of their physical/chemical properties and interaction with the underlying inorganic substrate. These hybrid interfaces have already found successful applications in the fields of photovoltaics,[5,6] energy harvesting[7] and sensing.[8] Metal-tetraphenylporphyrins (MTPP) are promising candidates for perspective applications in organic electronics, due to the possibility of fine tuning their electronic[9] and magnetic[10] properties by following several synthetic approaches[11,12] and by selecting the metal ion to be placed inside the macrocycle cavity.[13] The porphyrin macrocycle is characterized by a planar structure showing only a slight saddle-like distortion.[10] The MTPP planarity can be considered an advantage since it allows for a direct interaction with the inner metallic ion; however, the planar structure may also enhance the coupling with the substrate and lead to the

perturbation of the electronic properties of the molecule.[14,15] Indeed, when a thin organic layer is deposited on top of a reactive substrate, such as Fe,[16] Cu[17] or Al,[18] the molecular properties can be severely altered. Even on a relatively inert substrate like Ag, however, the presence of the metallic surface can affect the chemical activity of the metal ion by acting as an additional ligand in those chemical reactions involving a bond with another molecular species (this is called the surface trans effect, STE[19]).

A possible strategy to circumvent this problem is to grow these molecules on top of a low interacting substrate[20,21] or to decouple the organic film from the electrode underneath by exploiting, *e.g.*, a graphene inter-layer[22] or a thin oxide layer.[23] In this respect, we have shown that the Fe(001) surface passivated with a ultra-thin iron oxide layer, namely Fe(001)–$p(1 \times 1)$O, is a good candidate for weakening the coupling between iron and porphyrins also avoiding, under certain circumstances, STE.[24,25] Indeed, we found that (i) the thin oxide allows enough molecular mobility to obtain an ordered and commensurate 2D porphyrin wetting layer,[16,26] (ii) the molecular features (especially the HOMO and LUMO states) are preserved[27] and (iii) a magnetic coupling between the organic film and the substrate is possible even at room temperature (RT).[13] Recently, we have also proved that this regular array of molecules can be used as a template for the growth of 3D molecular structures.[25] A crucial point regarding the MTPP/Fe(001)–$p(1 \times 1)$O interface is the robustness of the 2D molecular arrangement when non-planar molecules are employed in the formation of the organic layer. Nowadays, such kind of

[a] *Dipartimento di Fisica, Politecnico di Milano, p.za Leonardo da Vinci 32, 20133, Milano, Italy. E-mail: alberto.calloni@polimi.it*

[b] *Istituto Officina dei Materiali – CNR-IOM, Laboratorio TASC, s.s. 14 km 163.5, 34149 Trieste, Italy*

[c] *Dipartimento di Chimica, Università di Pavia, via Taramelli 12, 27100 Pavia, Italy*

[d] *Istituto di Scienze e Tecnologie Chimiche "G. Natta" del Consiglio Nazionale delle Ricerche (CNR-SCITEC), PST via G. Fantoli 16/15, 20138 Milano, Italy*

[e] *ETSF and Dipartimento di Fisica "Aldo Pontremoli", Università degli Studi di Milano, Via Celoria, 16, 20133 Milano, Italy*

This journal is © the Owner Societies 2022

Phys. Chem. Chem. Phys., 2022, **24**, 17077–17087 | **17077**

molecules (VO^{2+} porphyrins,[28] VO^{2+} and TiO^{2+} phthalocyanines,[29,30] *etc.*) find many applications related to the control of band-alignment at the electrode surface,[31] in dye-synthetized solar cells,[32] electrets,[33] *etc.* Metal-porphyrins with an anion bound to the coordinated metallic ion are no longer planar since the anion protrudes outside the macrocycle plane.[34,35] However, the distortion of the main porphyrin macrocycle could affect the assembling properties of such molecules and compromise their long-range ordering. A negligible substrate interaction and a long range ordering are important conditions in view of applications. Indeed, given the actual technological limitations in the nanoscale manipulation of molecular objects, the most likely strategy that will lead to the production of usable electronic devices exploiting the peculiar electronic characteristics of isolated molecules (single molecule devices)[36] foresees the use of ordered ensembles of molecules. The latter ones can be addressed either individually or collectively, so that the electric behavior of the related device can be simply scaled with the number of molecular units involved.[37]

In this paper, we have focused our attention on VOTPP molecules (see Fig. 1), in order to evaluate the role of the molecular non-planarity in the formation of a well-ordered molecular array and in their interaction with the substrate with respect to planar MTPPs.

Materials and methods

The preparation and the analysis of the samples are performed in vacuum chambers operating in the low 10^{-10} mbar regime.[38] The substrate was prepared following standard procedures reported in literature.[39] The Fe(001) surface is sputtered with 1.5 keV Ar$^+$ ions and then annealed at 480 °C for 10 minutes. Then, it is exposed to 30 L of molecular oxygen (being 1 L = 10^{-6} Torr s) with the sample kept at 450 °C. A subsequent flash at around 700 °C removes the excess of the deposited oxygen, resulting in the formation of a single (1×1) iron oxide layer. Its quality was verified by using Low Energy Electron Diffraction (LEED) and Photoemission Spectroscopy (PES). The organic deposition is accomplished in a dedicated chamber, with the

substrate kept at room temperature. Molecules are evaporated from a Knudsen cell ($T = 320$ °C); the flux rate was monitored by a quartz microbalance and maintained below 1 Å min^{-1}. The deposited thickness is evaluated in monolayers (ML), being 1 ML = 3.06 Å.

The porphyrin superstructure is analyzed by LEED. The organic film electronic structure below the Fermi energy (E_F) is studied by means of Ultraviolet PES (UPS). The photon source is a UV lamp producing HeI radiation ($h\nu = 21.2$ eV), while photoelectrons were collected by an hemispherical electron analyzer operated at a pass energy of 0.7 eV, yielding a full width at half maximum (FWHM) energy resolution of 15 meV.[15] A transmission optimized focusing mode (angular acceptance up to $\pm 9°$) was selected for the UPS measurements, acquired at normal electron emission. Given the relatively large molecular superstructure observed on the Fe(001)–$p(1 \times 1)$O surface ($a_{VOTPP} = 5a_{Fe}$, as detailed in the following), resulting in a very narrow surface Brillouin zone (BZ), the presented UPS results are representative of the VOTPP electronic structure averaged over the entire BZ, *i.e.* no spectral modifications are expected by changing the angle of electron emission (see, *e.g.* our previous results on 1 ML CoTPP on Fe–$p(1 \times 1)$O[26]). The electronic structure above the E_F is addressed by Inverse Photoemission Spectroscopy (IPES), operated in the isochromatic mode. The electron source is a GaAs photocathode, which undergoes a standard treatment to reach the negative electron affinity condition.[40] The emitted photon flux is collected by a detector with a band-pass filter centered at 9.6 eV. The FWHM energy resolution of the IPES experiment is 700 meV.[41]

To investigate the orientation of the molecules with respect to the substrate, we have employed near edge X-ray adsorption fine structure (NEFAFS), performed at the ALOISA beamline (Elettra synchrotron facility in Trieste, Italy).[42] The absorption spectra have been collected at two different orientations of the surface with respect to the linear polarization vector of the synchrotron photon beam, namely Transverse Magnetic (TM, closely p-polarization) and Transverse Electric (TE, s-polarization) geometry, by sample rotation around the photon beam axis at constant grazing angle $\alpha = 6°$. By the selection rules, the electron excitation from an s-symmetry core level (C 1s and N 1s) to an empty molecular orbital is maximum when the electric field is oriented along the orbital dipole. When molecules display a preferential orientation with respect to the surface, the corresponding π^* and σ^* symmetry resonances will display an opposite polarization dependence of their intensity (NEXAFS dichroism). In our scattering geometry, for a four-fold symmetry substrate, the ratio between the resonance intensity of a π-symmetry orbital (such as the aromatic rings of the phenyls, pyrroles and the whole hetero-aromatic macrocycle) measured in TE and TM polarization (I_{TE}/I_{TM}) is proportional to $1/2 \cdot \tan^2 \gamma$, where γ is the average tilt angle,[43] and we have assumed $\cos^2 \alpha \simeq 1$ and $\sin^2 \alpha \simeq 0$. The spectra are acquired in partial electron yield mode with a channeltron electron multiplier, equipped with a negatively biased grid filtering out secondary electrons (set to -230 V and -370 V for the C and N K-edges, and to -470 V for the V L-edge) to maximize the

Fig. 1 Schematic representation of a vanadyl-tetraphenyl porphyrin (R = phenyl group). (a) Top view; (b) 3D perspective view highlighting the orientation of the V–O bond along a direction perpendicular to the plane of the tetrapyrrolic ring.

17078 | *Phys. Chem. Chem. Phys.*, 2022, **24**, 17077–17087

This journal is © the Owner Societies 2022

signal-to-noise ratio. We performed absolute energy calibration of the C, N and V NEXAFS by simultaneous acquisition of the drain current on the surface (Au) of the last refocusing mirror, where the absorption lines of residual C, N and O contamination are calibrated by the reference X-ray absorption vibrational states measured in gas phase (287.40 eV, 401.10 eV, and 534.21 eV from CO and N_2) with a window-less gas ionization cell.[44] Finally, the NEXAFS spectra were normalized to reference NEXAFS spectra measured in the same conditions on the clean Fe–$p(1 \times 1)$O surface before deposition. At the ALOISA beamline, we performed complementary X-ray photoemission (XPS) measurements by means of a homemade hemispherical analyzer (mean radius of 66 mm, acceptance angle of $\sim 2°$, FWHM) equipped with a 2D-delay line detector (developed by Elettra). The XPS spectra have been measured in normal emission with the sample kept at a grazing angle $\alpha = 4°$ in TM polarization. We selected a photon energy of 650 eV to measure the V 2p spectra (overall resolution of 260 meV).

In view of having a rationale of the collected data, we have analyzed the system by *ab initio* calculations within density functional theory (DFT), using for exchange and correlation the vdW-DF-c09 functional,[45] which takes into account dispersion forces. We use the Quantum ESPRESSO simulation package[46,47] that implements periodically repeated cells, ultrasoft pseudo-potentials and plane waves. For pseudopotentials, we used the same as in our previous publication on CoTPP/Fe(001)–$p(1 \times 1)$O,[15]

namely we have taken files generated from scalar-relativistic all-electron calculations, as available from the Quantum-ESPRESSO website for Fe and O (as in ref. 48) and V, and from pslibrary[49] for Ni, H, C and N. The cutoff for plane wave expansion was set to 36 Ry and to 220 Ry for the wavefunctions and electron density, respectively. The model of the Fe(001)–$p(1 \times 1)$O substrate consists in a four-layer Fe slab, where the bottom two are fixed at the bulk interlayer distance and O is adsorbed on the top side as in our previous works.[48] We sample the Brillouin zone of the supercell adopted in the calculation by a 2×2 shifted Monkhorst–Pack grid[50] that would corresponds to a 10×10 sampling in the surface Brillouin zone of Fe(001). Geometry optimization of molecular coordinates is then performed until the forces on atoms are lower than 0.1 mRy bohr^{-1}. We include the DFT + U correction for V atoms to improve the treatment of on-site correlation. We consider the rotationally-invariant form with a single parameter $U_{eff} = U - J = 3.0$ eV, resulting from $U = 4.0$ eV and $J = 1.0$ eV.[9,51–53] We have verified previously that calculations without the +U correction yield very similar adsorption energies and coordinates,[54] whereas they would result in metal 3d states too close to E_F.

Results and discussion

The spectra acquired on the VOTPP/Fe–$p(1 \times 1)$O system by UPS and IPES are displayed in Fig. 2. The photoemission signal

Fig. 2 UPS (left) and IPES (right) spectra acquired on the Fe–$p(1 \times 1)$O substrate and after the growth of 1 and 20 ML thick VOTPP layers. Photoemission features from O and Fe species are highlighted in the substrate spectra, while labels (R) and (Ph) account for photoemission from the VOTPP macrocycle and peripheral phenyl groups, respectively.

This journal is © the Owner Societies 2022

Phys. Chem. Chem. Phys., 2022, **24**, 17077–17087 | **17079**

from the substrate shows features from (i) Fe 3d states close to E_F, qualitatively similar to those observed on Fe(001),[16,39] and (ii) O species at an energy of about -4.5 eV. The spectra from the 20 ML film can be considered as representative of photoemission from not-interacting or weakly bonded (*via* van der Waals interactions) VOTPP molecules.[55] Photoemission features from the substrate are greatly attenuated; we can thus associate each visible peak in Fig. 2 with to photoemission from either the macrocycle (R) or the phenyl groups (Ph), according to a comparison between the simulated spectra for metal-tetraphenylporphyrins and metal-porphyrins (without phenyl terminations) in the literature.[56] Conversely, the spectra from the VOTPP monolayer feature some overlapping signal from the substrate, especially close to E_F (Fe 3d orbitals). No contribution is instead expected from the photoemission feature from O 2p states, quenched at ML coverage as reported in other literature works on MTPP growth on Fe–$p(1 \times 1)$O.[16] Given the similarity of the spectra from the thin VOTPP single layer and the thicker one, it is possible to assign a common spectroscopic origin to those features appearing in both (connected through vertical dotted lines). We exclude the occurrence of a strong chemisorption at the molecule/oxide interface, that would likely lead to a significant perturbation of the highest occupied and lowest unoccupied molecular orbitals (HOMO and LUMO orbitals, respectively) as observed instead on our previous work on MTPP growth on clean Fe(001).[16,57] The 20 ML VOTPP film is characterized by a HOMO–LUMO gap of 4.1 ± 0.3 eV, evaluated by considering the centroid of the HOMO R_1 feature and the LUMO R peak, after the removal of a rising background. The reported VOTPP optical gap[58] is about 2 eV smaller than the above value, mainly accounting for the energy released upon exciton formation during the optical excitation.[56] The observed reduction of the peak-to-peak gap in the ML film (down to about 3 eV, with the position of the LUMO R peak computed according to ref. 59) mostly originates from the enhanced screening of the photogenerated hole (added electron) in UPS (IPES) in close proximity to the metallic Fe surface, as observed in other MTPP/Fe–$p(1 \times 1)$O systems.[15] The Fermi energy is close to the upper edge of the electronic gap, suggesting a n-type behaviour of the VOTPP layer. The proper assessment of the electrical behaviour of the molecular film would require further investigation; however, a strong influence of the substrate's work function on band alignment at the molecule/substrate interface is expected, rather than an intrinsic doping of the film, favouring electron injection into the molecular film.[60]

In Fig. 3 is shown the LEED pattern characteristic of the 1 ML VOTPP/Fe–$p(1 \times 1)$O system. The ordered pattern we obtained resembles what already observed on 1 ML of CoTPP[27] and NiTPP[24] layers grown on top of Fe(001)–$p(1 \times 1)$O. By using a LEED simulator (LEEDpat[61]), we interpret the diffraction pattern as due to a commensurate (5×5) superstructure that exhibits two domains rotated by $37°$ ($R37$) with respect to substrate $\langle 001 \rangle$ high-symmetry directions. The presence of an ordered superstructure [not observed when VOTPP are evaporated on the bare Fe(001) substrate] confirms that the weak coupling provided by the thin oxide layer is efficient in
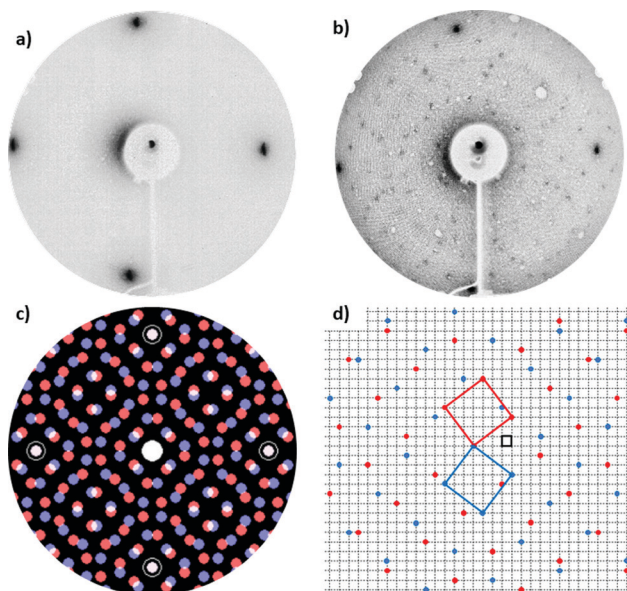

Fig. 3 LEED pictures acquired with a beam energy of 55 eV on (a) the Fe–$p(1 \times 1)$O and (b) the 1 ML VOTPP/Fe–$p(1 \times 1)$O surface. (c) LEEDpat simulation of the expected LEED pattern for the (5×5) $R37$ 1 ML VOTPP superstructure. (d) Real space schematics of the corresponding two molecular domains formed on top of the substrate. The VOTPP lattice unit cell (red and blue rectangles represent the two possible orientations) is 5×5 times larger than the substrate one (black grid).

fostering the molecules mobility, regardless of the presence of the distorted porphyrin molecular skeleton. From the photoemission and diffraction data reported above, we can state that VOTPP molecules behave similarly to the standard, planar MTPP molecules, which arrange in a regular array on top of the substrate and keep their semiconductive properties.

Non-planar metal-porphyrins can have their main ring tilted with respect to the substrate, thus precluding the orientation of the molecular skeleton parallel to the surface. The latter configuration is preferred to enhance the possible interaction of the metallic ion core (the MTPP coordination site) with the surroundings. NEXAFS spectroscopy allows us to explore the average molecular orientation and conformation in the grown film by considering the differences in the absorption spectra acquired with s- and p-polarized light. In Fig. 4, the NEXAFS spectra acquired at the N K-edge and C K-edge are reported, together with a schematic of the adsorption geometry. In the upper panel, peak a can be assigned to the LUMO orbital, while peaks b–e to higher-energy unoccupied orbitals.[62] According to theory, due to the LUMO orbital $\pi^\star$-symmetry, a different absorption of s- and p-polarized light gives clues about the molecule orientation with respect to the substrate. In the present case, the strong dichroism characterizing the sample, with the first four peaks (a, b, c, d) visible only with p-polarized light, indicates that the tetrapyrrolic macrocycle lies almost perfectly flat on top of the substrate.[14] We note that the slight saddle-shape distortion of the porphyrin macrocycle, common in all MTPP,[10] is expected to give only minor contributions (few % of residual intensity in s-polarization) to the NEXAFS signal.[63]

17080 | *Phys. Chem. Chem. Phys.*, 2022, **24**, 17077–17087
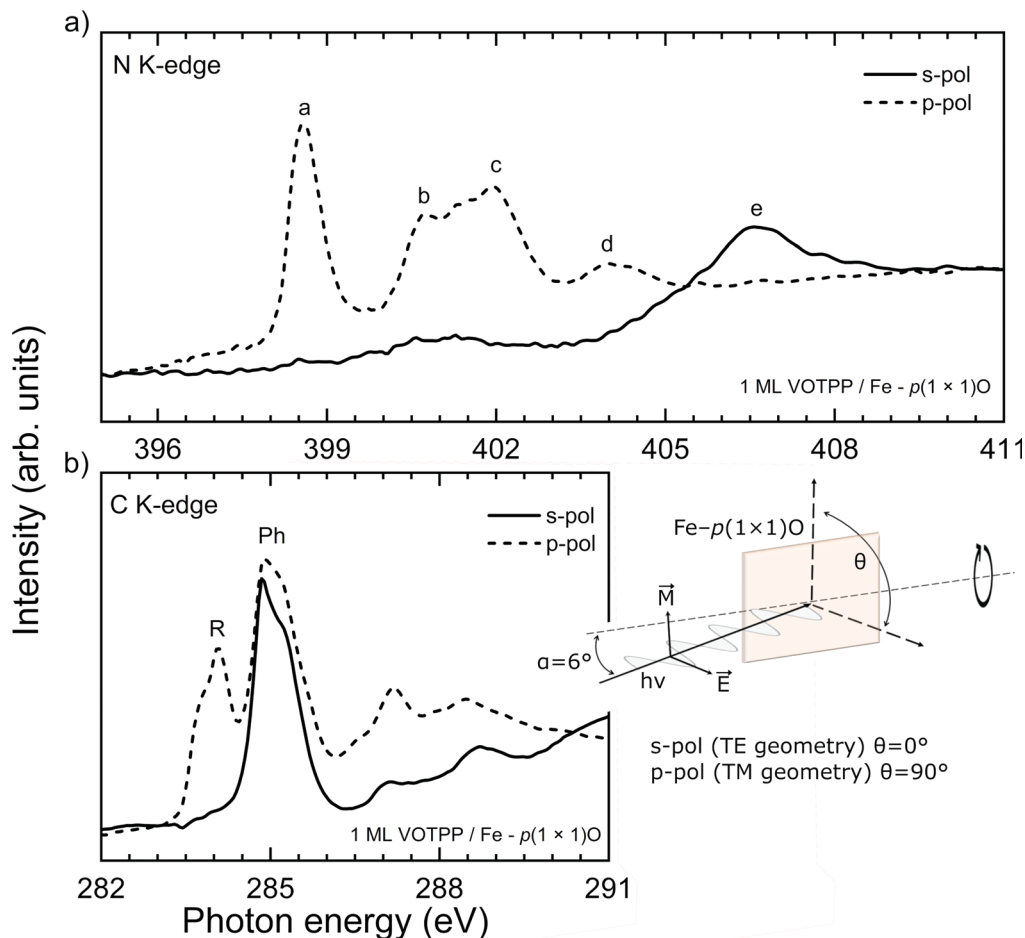
This journal is © the Owner Societies 2022

Fig. 4   (a) NEXAFS at the N K-edge for the system 1 ML VOTPP/Fe−$p(1 \times 1)$O. The spectrum acquired with s (p) polarization is shown with a full (dashed) line. The spectral features are labelled according to previous works.[15] (b) NEXAFS at the C K-edge for the system 1 ML VOTPP/Fe−$p(1 \times 1)$O. The spectrum acquired with s (p) polarization is shown with a full (dashed) line. The spectral features are labelled with R (Ph) when they are attributed to the tetrapyrrolic ring (phenyl groups) of the molecule. A schematic is added to illustrate the substrate orientation with respect to the X ray beam, as also explained in the materials and methods section.

Our results therefore convey an important message: the presence of the protruding oxygen atom does not affect the orientation of the macrocycle on top of the substrate, nor enhances its saddle-like distortion. A confirmation arises from the C K-edge NEXAFS spectra shown in the lower panel of Fig. 4; the peaks are labelled according to the literature.[64] While the Ph-peak does show a minor and reversed dichroism, suggesting that the peripheral groups are tilted off the surface by 55°–60°, the R-feature appears only in p-polarization (main tetrapyrrolic ring parallel to the surface).

Fig. 5 shows the NEXAFS (panel a) and XPS (panel b) results collected at the V $L_{2,3}$-edges and in the V 2p binding energy region, respectively, on 1 ML VOTPP/Fe−$p(1 \times 1)$O and a multilayer (3 ML thick) VOTPP film on Fe−$p(1 \times 1)$O. The observed features are related to electronic transitions from 2p to empty 3d states. Electron excitations in 3d states with a predominant character in(out) of the surface plane are probed with s(p)-light. The strong dichroism observed in Fig. 5a on the L_3 edge and the absorption lineshape are compatible with the results reported in ref. 65 for thin films of flat lying vanadyl

phthalocyanines on graphene/Ni(111) and consistent with the information obtained from the analysis of K-edge data (Fig. 4). An unresolved signal is observed at the L_2 edge due to the broadening induced by the shorter lifetime of the core hole.[66]

The 1 ML spectra display the same NEXAFS resonances as the multilayer, which is a strong indication that the electronic structure of the macrocycle is not significantly affected by the proximity of the substrate, apart from a small decrease of the lifetime of unoccupied MOs, as witnessed by the broadening of the resonances with respect to the multilayer. The V atom has a formal valence of 4+, resulting in the occupation of a single 3d orbital. A significant interaction with the core hole is therefore expected in the final state of both NEXAFS and XPS, leading to the multiplet splitting of the spectroscopic features.[67] Slight changes in the multiplet fine structure of the V $2p_{3/2}$ peak in Fig. 5b might account for the observed differences in the reported spectra, together with a general broadening of the spectroscopic features for the monolayer film. We hardly detected any significant variation of the V $2p_{3/2}$ peak centroid position, as can be appreciated in the point-by-point difference
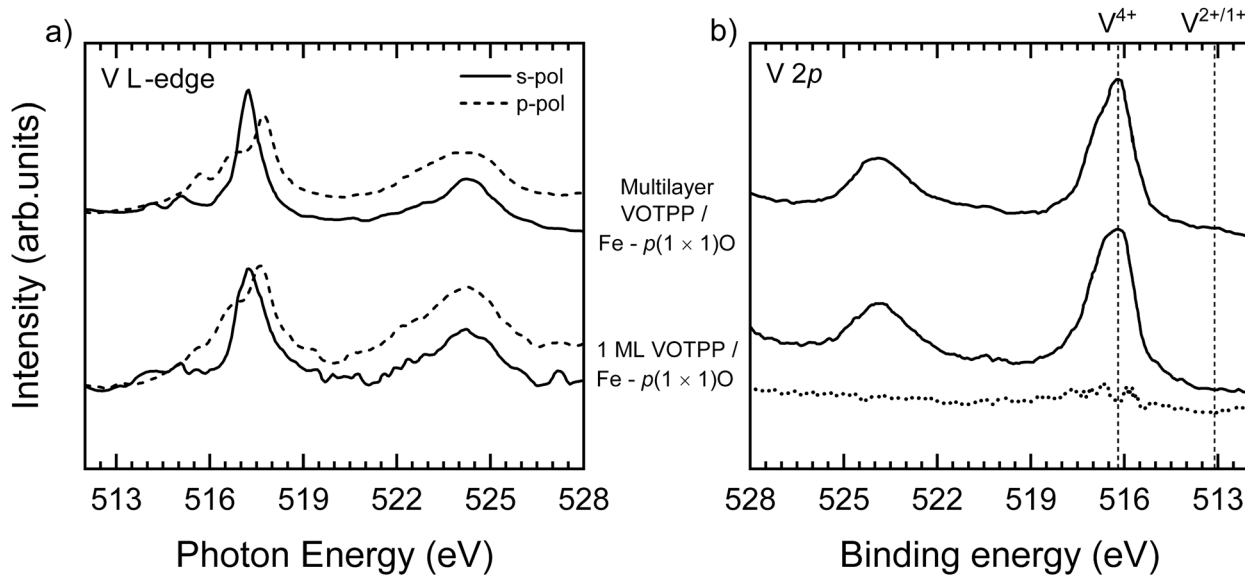
Fig. 5 (a) NEXAFS spectra acquired at the V $L_{2,3}$-edges and (b) high resolution XPS spectra in the V 2p binding energy range for a single and multilayer VOTPP film on Fe-$p(1 \times 1)$O. Spectra acquired with s- (p-)polarized light is presented with full (dashed) lines in panel (a). In panel (b), vertical dashed lines mark the binding energy position of photoemission features from V^{4+} and $V^{2+/1+}$ species.[67] The point-by-point difference between the multilayer and the monolayer spectra is reported with a dotted line.

between the two spectra (Fig. 5b, dotted line). This suggests a negligible interaction between the V atom and the substrate.[68] The vertical lines at 516.2 eV and 513.1 eV in Fig. 5b mark the binding energy position of the photoemission features from V^{4+} and $V^{2+/1+}$ species, as reported in ref. 67 for VOTPP and VTPP molecules, respectively. The absence of any feature related to VTPP in our spectra excludes the occurrence of a V–O bond cleavage in our samples, contrary to the case of VOTPP deposition on the bare Fe(001) surface.[57]

The oxygen atom bound to the porphyrin molecules cannot be studied in detail to understand, for instance, its orientation and position with respect to the substrate, due to the presence of a relatively huge amount of oxygen in the underlying substrate contributing to the O signal in photoemission and adsorption spectra. To overcome this problem we performed a theoretical simulation to understand the most favorable VOTPP orientation when the molecules are deposited onto Fe(001)–$p(1 \times 1)$O. In the following, the molecular configuration with the VO^{2+} ion directed towards the substrate is labelled as Odwn, while Oup represents the configuration where VO^{2+} ion protrudes to the vacuum. In the Oup (Odwn) case, the V atom can be positioned either above a Fe atom or a substrate O atom; in view of distinguishing such configurations, we adopt the following lettering: Oup@Fe (Odwn@Fe), Oup@O (Odwn@O), respectively. The molecule can also attain two different in-plane orientations with respect to the lattice vectors of the (5×5)-$R37$ molecular superstructure, having different registry with the substrate. Here, we take into account only the specific in-plane azimuthal orientation that, for each adsorption site, corresponds to having the N atoms approximately above surface O as this is energetically preferred by ~ 0.3 eV, according to our previous calculations.[15] Fig. 6 reports

the Odwn@Fe and Oup@O configurations, taking as an example the overlayer as marked in red in Fig. 3c (the blue case is obtained by reflection).

The computed adsorption energies are reported in Table 1. The most stable configuration is that where the molecular V atom is placed above a Fe atom and its O-bonded atom points towards the surface, namely Odwn@Fe. The analysis of the electron density displacement with respect to the sum of the individual surface and molecule electron densities, shown in Fig. 6c, exhibits charge accumulation in the molecular O–substrate Fe region. On the contrary, the most stable configuration among those having O directed towards the vacuum finds VO^{2+} ion placed above an oxygen atom of the Fe(001)–$p(1 \times 1)$O surface (Oup@O). Despite being stabilized by the interaction of the macrocycle with the surface, this configuration shows a slightly higher energy with respect to the Odwn@Fe (+0.02 eV). As expected, the Odwn@O, which foresees the negatively charged porphyrin O atoms face-to-face with those of the substrate, is significantly less stable than all other cases.

In all the cases, the macrocycle lies almost flat on the surface, being slightly bent in the typical saddle shape common to other MTPPs. Therefore, the molecule does not tilt towards the surface, despite the VO^{2+} ion protrusion. In practice, we perform structural optimizations for molecules initially tilted along either of the two in-plane axes and observe that they recover an orientation parallel to the substrate. Regarding the molecular geometry, we find that the V atom stands out of the surrounding N atoms by about 0.50 Å (see z_V–z_N in Table 1). The O atom of the vanadyl cation further protrudes by 1.60 Å (computed for the free molecule). The VO^{2+} ion thus influences the distance of the molecular macrocycle (z_N in Table 1) with
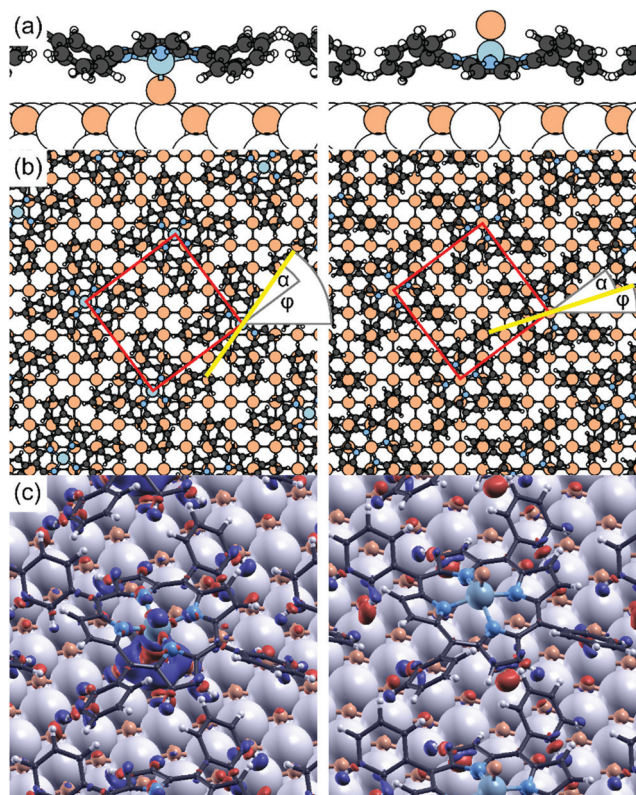
17082 | *Phys. Chem. Chem. Phys.*, 2022, **24**, 17077–17087

This journal is © the Owner Societies 2022

Fig. 6 (a) Side and (b) top view of the adsorption geometry of VOTPP in the Odwn@Fe and Oup@O configurations. Red squares indicate the (5×5)-$R37$ surface unit cell; oxygen and iron atoms are identified in orange and white, respectively. Yellow lines mark the N–N direction passing through the pyrrole rings bent inwards; ϕ and α are the angles formed by the red line with the [100] direction and with an overlayer lattice vector, respectively. (c) Electron density displacement upon adsorption (red: electron accumulation; blue: depletion), shown at the isovalue of ± 0.005 Å^{-3}.

Table 1 Adsorption energy of the four investigated VOTPP configurations, computed by DFT; height of the V atom (z_V) and average height of the N atoms (z_N) over the surface O plane

Configuration	Adsorption energy (eV)	Relative energy (eV)	z_V (Å)	z_N (Å)
Odwn@Fe	−4.21	0.00	3.26	3.70
Odwn@O	−3.34	0.87	3.90	4.31
Oup@Fe	−4.16	0.05	3.81	3.32
Oup@O	−4.19	0.02	3.68	3.21

respect to the buried substrate when the VO^{2+} ion is interposed between the porphyrin and the Fe(001)–$p(1 \times 1)$O in all the Odwn configurations. In the latter case, the two pyrrole rings towards the surface are more bent (19° vs. 13° in the Oup arrangements), while the other two pyrrole rings bend by 18° outwards in both cases. The Odwn@Fe electronic density of states (DOS) is reported in Fig. 7a, where the "+U" correction for V states is included. Overall, the shape of the DOS is in good agreement with the UPS/IPES spectra from Fig. 2, in particular concerning the position of phenyl-derived states, accounting for the energy-scale compression introduced by the DFT-GGA
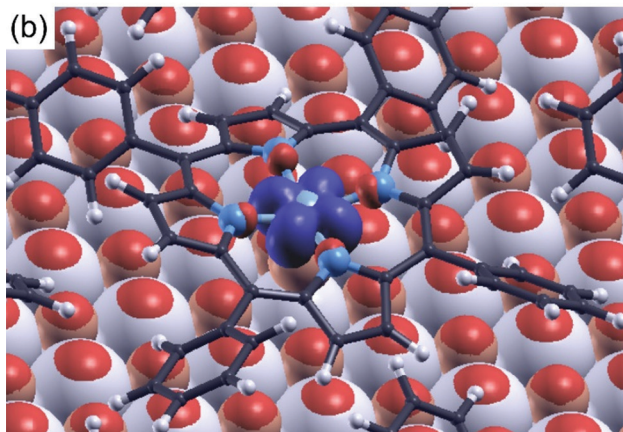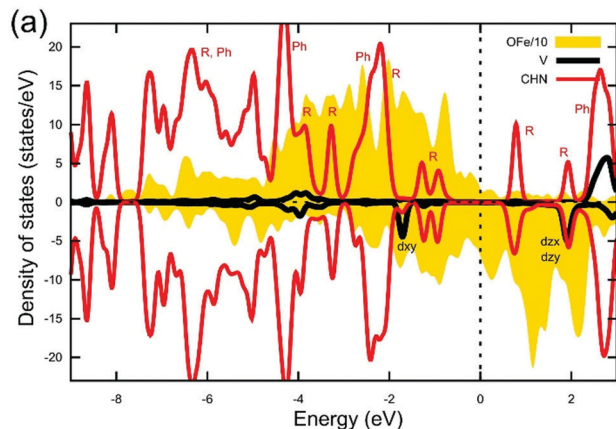

Fig. 7 (a) Projected density of states (DOS) of adsorbed VOTPP in the Odwn@Fe configuration (spin minority contributions are shown with negative sign). (b) Spin polarization of the system (difference between the spin-majority and spin-minority electron densities). The isovalue shown is ± 0.02 Å^{-3}.

formalism.[15] The HOMO–LUMO gap of 1.7 eV from the simulations is similarly smaller than the experimental one; in addition, the HOMO and LUMO are π states not involving the V atom. Around E_F, there are V contributions due to d$_{xy}$ orbital, at about −1.7 eV, and to d$_{xz}$/d$_{yz}$ orbitals coupled to O 2p states at +2 eV. Both the contributions are found in the minority spin channel. The singly occupied d$_{xy}$ state is responsible for the spin polarization of the molecule, antiparallel with respect to that of the substrate (see Fig. 6b). A similar DOS (not shown) is found for the Oup@O system arrangement, where minor differences are a direct consequence of the hybridization of the molecule, here standing at a shorter distance from the substrate. Considering the data of Table 1, we speculate that an ensemble of domains with VO^{2+} pointing downwards (Odwn@Fe) and upwards (Oup@O, Oup@Fe) is possible on the Fe(001)–$p(1 \times 1)$O surface, similarly to previous findings for chloroaluminum phthalocyanine on Au(111).[69]

Conclusions

The investigation of MOTPP properties when these molecules are grown on top of a passivated metal surface [namely

Fe(001)–$p(1 \times 1)$O] is of primary importance, since they can be exploited as a functionalized template, interesting for catalysis or for the deposition of layered structures. In this respect, a non-planar porphyrin (namely, VOTPP) can represent a suitable choice due to the preferential interaction site (VO^{2+} ion) carried by the molecule itself. However, the presence of the VO^{2+} cation, protruding from the molecular plane, can have possible drawbacks in the assembling of such kind of molecules. For this reason, we performed a NEXAFS and photoemission characterization of VOTPP layers deposited on Fe(001)–$p(1 \times 1)$O, and compared the results to previous analyses performed on planar porphyrin molecules (such as Co and NiTPP). Our results highlight that the non-planar configuration does not affect *a priori* the assembling properties of the organic film. (i) VOTPP arrange themselves in an ordered and commensurate 5×5 configuration, similar to that of Co and NiTPPs on the same surface; (ii) the VOTPP macrocycle lies flat and parallel with respect to the substrate, without any evidence of tilting. In addition, the coupling with the thin metal-oxide layer is weak, with the possibility for the molecule to exhibit the HOMO–LUMO features at a single layer coverage, even on a strongly reactive surface such as the one of Fe(001). Important information also arises from theoretical calculations, suggesting that an ensemble of VOTPP domains, where the VO^{2+} ion is directed either towards the substrate or the vacuum, is possible.

Author contributions

G. A. investigation, data curation and analysis, writing – original draft; L. S., F. G. and F. M. investigation, data analysis; A. C. validation, writing – review and editing; A. O. B. and A. B. conceptualization, validation, writing – review and editing; S. A. and G. F. investigation, data curation and analysis, validation, writing – review and editing; C. Z. writing – review and editing; L. F. investigation, supervision, validation, writing – review and editing; G. B. conceptualization, supervision, validation, writing – review and editing.

Conflicts of interest

There are no conflicts to declare.

Acknowledgements

References

1 *Hybrid Organic-Inorganic Interfaces: Towards Advanced Functional Materials*, ed. M.-H. Delville and A. Taubert, Wiley-VCH Verlag GmbH & Co. KGaA, 2018.

2 G. Witte and C. Wöll, Growth of aromatic molecules on solid substrates for applications in organic electronics, *J. Mater. Res.*, 2004, **19**, 1889–1916.

3 C. Barraud, P. Seneor, R. Mattana, S. Fusil, K. Bouzehouane, C. Deranlot, P. Graziosi, L. Hueso, I. Bergenti, V. Dediu, F. Petroff and A. Fert, Unravelling the role of the interface for spin injection into organic semiconductors, *Nat. Phys.*, 2010, **6**, 615–620.

4 M. Callsen, V. Caciuc, N. Kiselev, N. Atodiresei and S. Blügel, Magnetic hardening induced by nonmagnetic organic molecules, *Phys. Rev. Lett.*, 2013, **111**, 106805.

5 B. W. D'Andrade, A. Z. Kattamis and P. F. Murphy, *Flexible organic electronic devices on metal foil substrates for lighting, photovoltaic, and other applications*, Elsevier Ltd, 2015.

6 S. M. Zegeye, A review paper on spintronics and its role to improve electronic devices, *Am. J. Quantum Chem. Mol. Spectrosc.*, 2019, **3**, 41–47.

7 R. Guterman, J. Yuan, L. Sobhana, P. Fardim, S. Garcia-Mayo and G. Salazar-Alvarez, in *Hybrid Organic-Inorganic Interfaces: Towards Advanced Functional Materials*, ed. M.-H. Delville and A. Taubert, Wiley-VHC, 2018, pp. 199–240.

8 L. De Stefano, I. Rea, I. Rendina, M. Giocondo, S. Houmadi, S. Longobardi and P. Giardina, in *Biosensors – Emerging Materials and Applications*, ed. P. A. Serra, 2011, pp. 311–332.

9 M. S. Liao and S. Scheiner, Electronic structure and bonding in metal phthalocyanines, metal = Fe, Co, Ni, Cu, Zn, Mg, *J. Chem. Phys.*, 2001, **114**, 9780.

10 J. M. Gottfried, Surface chemistry of porphyrins and phthalocyanines, *Surf. Sci. Rep.*, 2015, **70**, 259–379.

11 J. S. Lindsey, Synthetic routes to meso-patterned porphyrins, *Acc. Chem. Res.*, 2010, **43**, 300–311.

12 M. O. Senge, Stirring the porphyrin alphabet soup—functionalization reactions for porphyrins, *Chem. Commun.*, 2011, **47**, 1943.

13 M. S. Jagadeesh, A. Calloni, A. Brambilla, A. Picone, A. Lodesani, L. Duò, F. Ciccacci, M. Finazzi and G. Bussetti, Room temperature magnetism of ordered porphyrin layers on Fe, *Appl. Phys. Lett.*, 2019, **115**, 082404.

14 A. Picone, D. Giannotti, A. Brambilla, G. Bussetti, A. Calloni, R. Yivlialin, M. Finazzi, L. Duò, F. Ciccacci, A. Goldoni, A. Verdini and L. Floreano, Local structure and morphological evolution of ZnTPP molecules grown on Fe(001)–$p(1 \times 1)$O studied by STM and NEXAFS, *Appl. Surf. Sci.*, 2018, **435**, 841–847.

15 A. Calloni, M. S. Jagadeesh, G. Bussetti, G. Fratesi, S. Achilli, A. Picone, A. Lodesani, A. Brambilla, C. Goletti, F. Ciccacci, L. Duò, M. Finazzi, A. Goldoni, A. Verdini and L. Floreano, Cobalt atoms drive the anchoring of Co-TPP molecules to the oxygen-passivated Fe(001) surface, *Appl. Surf. Sci.*, 2020, **505**, 144213.

16 G. Bussetti, A. Calloni, M. Celeri, R. Yivlialin, M. Finazzi, F. Bottegoni, L. Duò and F. Ciccacci, Structure and electronic properties of Zn-tetra-phenyl-porphyrin single- and multi-layers films grown on Fe(001)–$p(1 \times 1)$O, *Appl. Surf. Sci.*, 2016, **390**, 856–862.

17 M. S. Dyer, A. Robin, S. Haq, R. Raval, M. Persson and J. Klimeš, Understanding the interaction of the porphyrin

17084 | *Phys. Chem. Chem. Phys.*, 2022, **24**, 17077–17087

This journal is © the Owner Societies 2022

macrocycle to reactive metal substrates: Structure, bonding, and adatom capture, *ACS Nano*, 2011, **5**, 1831–1838.

18 A. Ruocco, F. Evangelista, R. Gotter, A. Attili and G. Stefani, Evidence of charge transfer at the Cu-phthalocyanine/Al(100) interface, *J. Phys. Chem. C*, 2008, **112**, 2016–2025.

19 W. Hieringer, K. Flechtner, A. Kretschmann, K. Seufert, W. Auwärter, J. V. Barth, A. Görling, H.-P. Steinrück and J. M. Gottfried, The surface trans effect: Influence of axial ligands on the surface chemical bonds of adsorbed metalloporphyrins, *J. Am. Chem. Soc.*, 2011, **133**, 6206–6222.

20 Z. Q. Zou, L. Wei, F. Chen, Z. Liu, P. Thamyongkit, R. S. Loewe, J. S. Lindsey, U. Mohideen and D. F. Bocian, Solution STM images of porphyrins on HOPG reveal that subtle differences in molecular structure dramatically alter packing geometry, *J. Porphyrins Phthalocyanines*, 2005, **9**, 387–392.

21 C. Ruggieri, S. Rangan, R. A. Bartynski and E. Galoppini, Zinc(II) tetraphenylporphyrin adsorption on Au(111): An interplay between molecular self-assembly and surface stress, *J. Phys. Chem. C*, 2015, **119**, 6101–6110.

22 J. Mao, H. Zhang, Y. Jiang, Y. Pan, M. Gao, W. Xiao and H. J. Gao, Tunability of supramolecular kagome lattices of magnetic phthalocyanines using graphene-based moiré patterns as templates, *J. Am. Chem. Soc.*, 2009, **131**, 14136–14137.

23 G. Bussetti, G. Albani, A. Calloni, M. Sangarashettyhalli Jagadeesh, C. Goletti, L. Duò and F. Ciccacci, Persistence of the Co-tetra-phenyl-porphyrin HOMO-LUMO features when a single organic layer is grown onto Cu(110)-(2 × 1)O, *Appl. Surf. Sci.*, 2020, **514**, 145891.

24 G. Albani, A. Calloni, A. Picone, A. Brambilla, M. Capra, A. Lodesani, L. Duò, M. Finazzi, F. Ciccacci and G. Bussetti, An in-depth assessment of the electronic and magnetic properties of a highly ordered hybrid interface: The case of nickel tetra-phenyl-porphyrins on Fe(001)–p(1 × 1)O, *Micromachines*, 2021, **12**, 191.

25 A. Orbelli Biroli, A. Calloni, A. Bossi, M. S. Jagadeesh, G. Albani, L. Duò, F. Ciccacci, A. Goldoni, A. Verdini, L. Schio, L. Floreano and G. Bussetti, Out-Of-plane metal coordination for a true solvent-free building with molecular bricks: Dodging the surface ligand effect for on-surface vacuum self-assembly, *Adv. Funct. Mater.*, 2021, **31**, 2011008.

26 A. Calloni, M. S. Jagadeesh, G. Albani, C. Goletti, L. Duò, F. Ciccacci and G. Bussetti, Ordered assembling of Co tetra phenyl porphyrin on oxygen-passivated Fe(001): From single to multilayer films, *EPJ Web Conf.*, 2020, **230**, 00014.

27 G. Albani, A. Calloni, M. S. Jagadeesh, M. Finazzi, L. Duò, F. Ciccacci and G. Bussetti, Interaction of ultra-thin CoTPP films on Fe(001) with oxygen: Interplay between chemistry, order, and magnetism, *J. Appl. Phys.*, 2020, **128**, 035501.

28 T. A. Dar, R. Tomar, R. M. Mian, M. Sankar and M. R. Maurya, Vanadyl β-tetrabromoporphyrin: Synthesis, crystal structure and its use as an efficient and selective catalyst for olefin epoxidation in aqueous medium, *RSC Adv.*, 2019, **9**, 10405–10413.

29 N. A. Roslan, A. Abu Bakar, T. M. Bawazeer, M. S. Alsoufi, N. Alsenany, W. H. Abdul Majid and A. Supangat, Enhancing the performance of vanadyl phthalocyanine-based humidity sensor by varying the thickness, *Sens. Actuators, B*, 2019, **279**, 148–156.

30 X. F. Zhang, Y. Wang and L. Niu, Titanyl phthalocyanine and its soluble derivatives: Highly efficient photosensitizers for singlet oxygen production, *J. Photochem. Photobiol., A*, 2010, **209**, 232–237.

31 F. Widdascheck, A. A. Hauke and G. Witte, A solvent-free solution: Vacuum-deposited organic monolayers modify work functions of noble metal electrodes, *Adv. Funct. Mater.*, 2019, **29**, 1808385.

32 Q. Hu, E. Rezaee, M. Li, Q. Chen, Y. Cao, M. Mayukh, D. V. McGrath and Z. X. Xu, Molecular design strategy in developing titanyl phthalocyanines as dopant-free hole-transporting materials for perovskite solar cells: Peripheral or nonperipheral substituents?, *ACS Appl. Mater. Interfaces*, 2019, **11**, 36535–36543.

33 T. A. Ageeva, A. A. Bush, D. V. Golubev, A. S. Gorshkova, K. E. Kamentsev, O. I. Koifman, V. D. Rumyantseva, A. S. Sigov and V. V. Fomichev, Porphyrin metal complexes with a large dipole moment, *J. Organomet. Chem.*, 2020, **922**, 121355.

34 D. A. Duncan, P. S. Deimel, A. Wiengarten, M. Paszkiewicz, P. Casado Aguilar, R. G. Acres, F. Klappenberger, W. Auwärter, A. P. Seitsonen, J. V. Barth and F. Allegretti, Bottom-up fabrication of a metal-supported oxo-metal porphyrin, *J. Phys. Chem. C*, 2019, **123**, 31011–31025.

35 M. G. B. Drew, P. C. H. Mitchell and C. E. Scott, Crystal and molecular structure of three oxovanadium(IV) porphyrins: Oxovanadium tetraphenylporphyrin(I), oxovanadium(IV) etioporphyrin(II) and the 1:2 adduct of (II) with 1,4-dihydroxybenzene(III). Hydrogen bonding involving the VO group. Relevance to catalytic demetallisation, *Inorg. Chim. Acta*, 1984, **82**, 63–68.

36 A. Aviram and M. A. Ratner, Molecular rectifiers, *Chem. Phys. Lett.*, 1974, **29**, 277–283.

37 M. Jurow, A. E. Schuckman, J. D. Batteas and C. M. Drain, Porphyrins as molecular electronic components of functional devices, *Coord. Chem. Rev.*, 2010, **254**, 2297–2310.

38 G. Berti, A. Calloni, A. Brambilla, G. Bussetti, L. Duò and F. Ciccacci, Direct observation of spin-resolved full and empty electron states in ferromagnetic surfaces, *Rev. Sci. Instrum.*, 2014, **85**, 073901.

39 R. Bertacco and F. Ciccacci, Oxygen-induced enhancement of the spin-dependent effects in electron spectroscopies of Fe(001), *Phys. Rev. B*, 1999, **59**, 4207–4210.

40 I. V. Bazarov, B. M. Dunham, Y. Li, X. Liu, D. G. Ouzounov, C. K. Sinclair, F. Hannon and T. Miyajima, Thermal emittance and response time measurements of negative electron affinity photocathodes, *J. Appl. Phys.*, 2008, **103**, 054901.

41 M. Finazzi, A. Bastianon, G. Chiaia and F. Ciccacci, High-sensitivity bandpass UV photon detector for inverse photoemission, *Meas. Sci. Technol.*, 1993, **4**, 234–236.

42 L. Floreano, A. Cossaro, R. Gotter, A. Verdini, G. Bavdek, F. Evangelista, A. Ruocco, A. Morgante and D. Cvetko, Periodic arrays of Cu-Phthalocyanine chains on Au(110), *J. Phys. Chem. C*, 2008, **112**, 10794–10802.

This journal is © the Owner Societies 2022

Phys. Chem. Chem. Phys., 2022, **24**, 17077–17087 | **17085**

43 J. Stöhr, *NEXAFS Spectroscopy*, Springer-Verlag, Berlin, 1992.

44 L. Floreano, G. Naletto, D. Cvetko, R. Gotter, M. Malvezzi, L. Marassi, A. Morgante, A. Santaniello, A. Verdini, F. Tommasini and G. Tondello, Performance of the grating-crystal monochromator of the ALOISA beamline at the Elettra Synchrotron, *Rev. Sci. Instrum.*, 1999, **70**, 3855–3864.

45 T. Thonhauser, S. Zuluaga, C. A. Arter, K. Berland, E. Schröder and P. Hyldgaard, Spin signature of nonlocal correlation binding in metal-organic frameworks, *Phys. Rev. Lett.*, 2015, **115**, 136402.

46 P. Giannozzi, S. Baroni, N. Bonini, M. Calandra, R. Car, C. Cavazzoni, D. Ceresoli, G. L. Chiarotti, M. Cococcioni, I. Dabo, A. Dal Corso, S. De Gironcoli, S. Fabris, G. Fratesi, R. Gebauer, U. Gerstmann, C. Gougoussis, A. Kokalj, M. Lazzeri, L. Martin-Samos, N. Marzari, F. Mauri, R. Mazzarello, S. Paolini, A. Pasquarello, L. Paulatto, C. Sbraccia, S. Scandolo, G. Sclauzero, A. P. Seitsonen, A. Smogunov, P. Umari and R. M. Wentzcovitch, QUANTUM ESPRESSO: A modular and open-source software project for quantum simulations of materials, *J. Phys.: Condens. Matter*, 2009, **21**, 395502.

47 P. Giannozzi, O. Andreussi, T. Brumme, O. Bunau, M. B. Nardelli, M. Calandra, R. Car, C. Cavazzoni, D. Ceresoli and M. Cococcioni, *et al.*, Advanced capabilities for materials modelling with Quantum ESPRESSO, *J. Phys.: Condens. Matter*, 2017, **29**, 465901.

48 A. Picone, G. Fratesi, A. Brambilla, P. Sessi, F. Donati, S. Achilli, L. Maini, M. I. Trioni, C. S. Casari, M. Passoni, A. Li Bassi, M. Finazzi, L. Duò and F. Ciccacci, Atomic corrugation in scanning tunneling microscopy images of the Fe(001)–*p*(1 × 1) O surface, *Phys. Rev. B*, 2010, **81**, 115450.

49 A. Dal Corso, Pseudopotentials periodic table: From H to Pu, *Comput. Mater. Sci.*, 2014, **95**, 337–350.

50 H. J. Monkhorst and J. D. Pack, Special points for Brillouin-zone integrations, *Phys. Rev. B: Solid State*, 1976, **13**, 5188–5192.

51 A. M. Ritzmann, M. Pavone, A. B. Muñoz-García, J. A. Keith and E. A. Carter, *Ab initio* DFT+U analysis of oxygen transport in LaCoO$_3$: The effect of Co^{3+} magnetic states, *J. Mater. Chem. A*, 2014, **2**, 8060–8074.

52 S. J. Hu, S. S. Yan, M. W. Zhao and L. M. Mei, First-principles LDA + U calculations of the Co-doped ZnO magnetic semiconductor, *Phys. Rev. B: Condens. Matter Mater. Phys.*, 2006, **73**, 245205.

53 K. Leung, S. B. Rempe, P. A. Schultz, E. M. Sproviero, V. S. Batista, M. E. Chandross and C. J. Medforth, Density functional theory and DFT+U study of transition metal porphines adsorbed on Au(111) surfaces and effects of applied electric fields, *J. Am. Chem. Soc.*, 2006, **128**, 3659–3668.

54 G. Fratesi, S. Achilli, A. Ugolotti, A. Lodesani, A. Picone, A. Brambilla, L. Floreano, A. Calloni and G. Bussetti, Non-trivial central-atom dependence in the adsorption of M-TPP molecules (M = Co, Ni, Zn) on Fe(001)–*p*(1 × 1)O, *Appl. Surf. Sci.*, 2020, **530**, 147085.

55 C. Castellarin-Cudia, P. Borghetti, G. di Santo, M. Fanetti, R. Larciprete, C. Cepek, P. Vilmercati, L. Sangaletti, A. Verdini, A. Cossaro, L. Floreano, A. Morgante and A. Goldoni, Substrate influence for the Zn-tetraphenyl-porphyrin adsorption geometry and the interface-induced electron transfer, *ChemPhysChem*, 2010, **11**, 2248–2255.

56 S. Rangan, S. Katalinic, R. Thorpe, R. A. Bartynski, J. Rochford and E. Galoppini, Energy level alignment of a zinc(II) tetraphenylporphyrin dye adsorbed onto TiO$_2$(110) and ZnO(11$\bar{2}$0) surfaces, *J. Phys. Chem. C*, 2010, **114**, 1139–1147.

57 G. Albani, Molecules deposition on highly reactive surfaces: The case-study of porphyrins on Fe(001), *Il Nuovo Cimento C*, 2022, **45**, 157.

58 S. R. Stoyanov, C.-X. Yin, M. R. Gray, J. M. Stryker, S. Gusarov and A. Kovalenko, Computational and experimental study of the structure, binding preferences, and spectroscopy of nickel(II) and vanadyl porphyrins in petroleum, *J. Phys. Chem. B*, 2010, **114**, 2180–2188.

59 G. Bussetti, A. Calloni, R. Yivlialin, A. Picone, F. Bottegoni and M. Finazzi, Filled and empty states of Zn-TPP films deposited on Fe(001)–*p*(1 × 1)O, *Beilstein J. Nanotechnol.*, 2016, **7**, 1527–1531.

60 D. Yoshimura, H. Ishii, S. Narioka, M. Sei, T. Miyazaki, Y. Ouchi, S. Hasegawa, Y. Harima, K. Yamashita and K. Seki, The electronic structure of porphyrin/metal interfaces studied by UV photoemission spectroscopy, *Synth. Met.*, 1997, **86**, 2399–2400.

61 LEEDpat v.4.1 by K. E. Hermann and M. A. Van Hove, 2014, see: **http://www.fhi-berlin.mpg.de/KHsoftware/LEEDpat/**.

62 N. Schmidt, R. Fink and W. Hieringer, Assignment of near-edge X-ray absorption fine structure spectra of metallopor-phyrins by means of time-dependent density-functional calculations, *J. Chem. Phys.*, 2010, **133**, 054703.

63 A. Picone, D. Giannotti, A. Brambilla, G. Bussetti, A. Calloni, R. Yivlialin, M. Finazzi, L. Duò, F. Ciccacci, A. Goldoni, A. Verdini and L. Floreano, Local structure and morpho-logical evolution of ZnTPP molecules grown on Fe(001)–*p*(1 × 1)O studied by STM and NEXAFS, *Appl. Surf. Sci.*, 2018, **435**, 841–847.

64 K. Diller, F. Klappenberger, M. Marschall, K. Hermann, A. Nefedov, C. Wöll and J. V. Barth, Self-metalation of 2H-tetraphenylporphyrin on Cu(111): An X-ray spectroscopy study, *J. Chem. Phys.*, 2012, **136**, 014705.

65 H. Adler, M. Paszkiewicz, J. Uihlein, M. Polek, R. Ovsyannikov, T. V. Basova, T. Chassé and H. Peisert, Interface properties of VOPc on Ni(111) and graphene/Ni(111): Orientation-dependent charge transfer, *J. Phys. Chem. C*, 2015, **119**, 8755–8762.

66 D. Maganas, M. Roemelt, T. Weyhermüller, R. Blume, M. Hävecker, A. Knop-Gericke, S. DeBeer, R. Schlögl and F. Neese, L-edge X-ray absorption study of mononuclear vanadium complexes and spectral predictions using a restricted open shell configuration interaction ansatz, *Phys. Chem. Chem. Phys.*, 2014, **16**, 264–276.

17086 | *Phys. Chem. Chem. Phys.*, 2022, **24**, 17077–17087

This journal is © the Owner Societies 2022

67 P. S. Deimel, P. C. Aguilar, M. Paszkiewicz, D. A. Duncan, J. V. Barth, F. Klappenberger, W. Schöfberger and F. Allegretti, Stabilisation of tri-valent ions with a vacant coordination site at a corrole–metal interface, *Chem. Commun.*, 2020, **56**, 11219–11222.

68 M. Schmid, J. Zirzlmeier, H.-P. Steinrück and J. M. Gottfried, Interfacial interactions of iron(II) tetrapyrrole complexes on Au(111), *J. Phys. Chem. C*, 2011, **115**, 17028–17035.

69 Y. L. Huang, W. Chen, F. Bussolotti, T. C. Niu, A. T. S. Wee, N. Ueno and S. Kera, Impact of molecule-dipole orientation on energy level alignment at the submolecular scale, *Phys. Rev. B: Condens. Matter Mater. Phys.*, 2013, **87**, 085205.

This journal is © the Owner Societies 2022

Phys. Chem. Chem. Phys., 2022, **24**, 17077–17087 | **17087**